Technical Note 52537

The Role of Energy Resolution in Collecting World-Class Data for EDS

Keith Thompson, Thermo Fisher Scientific, Madison, WI, USA

Key Words

Active Detector Area, Collection Rate, EDS, Energy Dispersive Spectroscopy, Energy Resolution, Silicon Drift X-ray Detectors, Solid Angle

Introduction

Since the first Silicon Drift-based EDS detector (SDD) was commercially introduced roughly 15 years ago, X-ray detectors for energy dispersive spectroscopy (EDS) have undergone a wave of technology enhancements. The first such EDS systems featured an active area of 5 mm^2, an energy resolution between 160–200 eV and a maximum collection rate approaching only 100,000 input counts/second.

Commercially available SDD-based EDS detectors today feature active areas up to 150 mm^2 per device with multiple detectors commonly working in tandem. Collection rates of 1 million input counts/second are an expected standard. Spectral energy resolution down to 121 eV is now available. While energy resolution as measured and reported today is an important metric, it oversimplifies detector performance. When targeting actual end-user applications, a more in-depth evaluation and a much broader specification is required. This note addresses these issues.

Energy Resolution and the Entire Energy Spectrum

Energy resolution has approached its theoretical limit, which calls into question the importance of further advances in energy resolution.[1] Other factors or techniques may now play a more dominant role in collection of EDS data.

Figure 1 shows an EDS spectrum of a BN sample, whose surface was contaminated with C and O. An EDS spectrum of Be, whose surface was also contaminated with C and O is shown in Figure 2. These spectra show very clean and well-separated Be or B peaks, as well as N, C, and O peaks. The energy resolution for the EDS detector used to collect these data, as measured at Mn Kα, is 122 eV. The energy resolution of the C peak in both spectra is 39 eV.

Thermo SCIENTIFIC

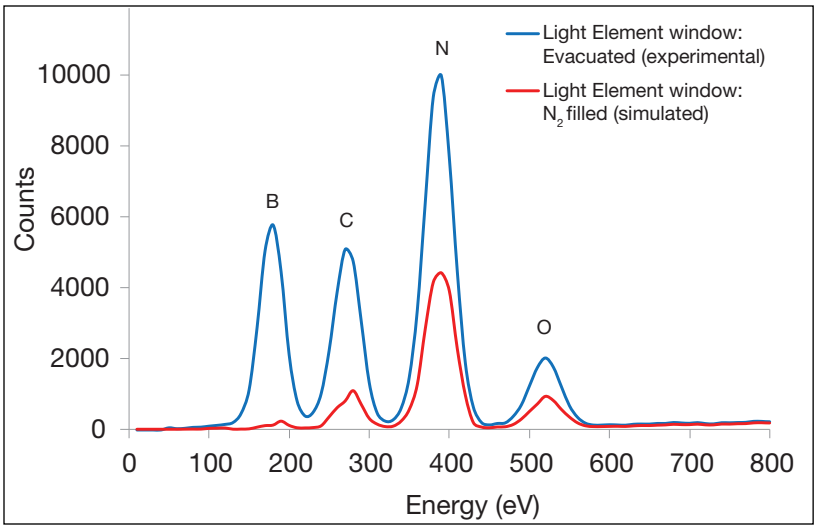

Figure 1: EDS spectrum of BN with C and O surface contamination as obtained with a fully evacuated EDS X-ray detector employing an ultra-thin, polymer window (blue) and the simulated spectrum if the detector module were back-filled with inert N_2 (red)

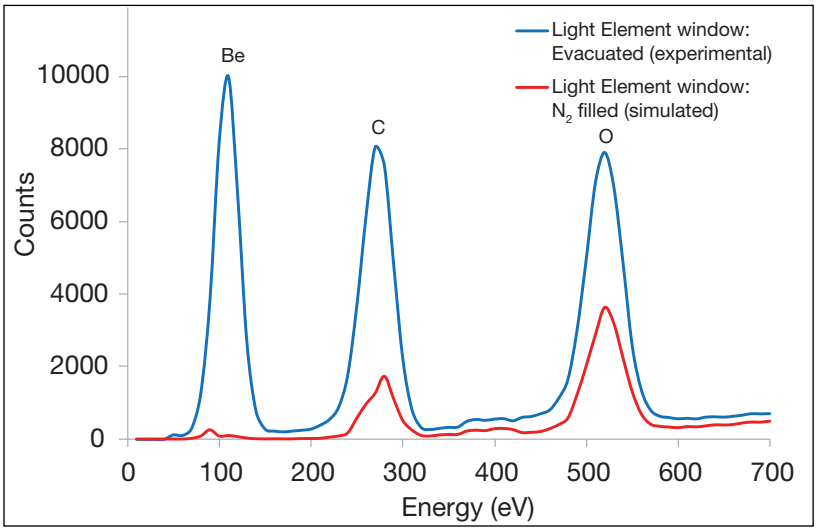

Figure 2: EDS spectrum of Be with C and O surface contamination as obtained with a fully evacuated EDS X-ray detector employing an ultra-thin, polymer window (blue) and the simulated spectrum if the detector module were back-filled with inert N_2 (red)

The advanced SDD represents only half of the improvement required to produce the spectra described above. Attenuation of low-energy X-rays seriously challenges low energy X-ray analysis. These X-rays are attenuated by many sources. First, the window used to isolate the SDD crystal from the microscope vacuum (or ambient while vented) absorbs low energy X-rays. Traditional Be windows prevent transmission of X-rays lower than the Na Kα line (~1 keV) and should therefore be eliminated as an option. Second, any inert gas between the SDD crystal and the window will absorb low energy X-rays. In many designs inert N_2 gas is intentionally used to back-fill the volume between the SDD crystal and the light-element window. The degradation of low-energy sensitivity by inert N_2 gas can be simulated by applying the X-ray absorption curves for N_2 gas across the distance the X-rays must travel through the N_2 gas. These simulated spectra are plotted in Figures 1 and 2. When compared against a detector whose volume is fully evacuated, as opposed to back-filled with N_2, the difference in low energy sensitivity is stark. Finally, the sample itself absorbs low energy X-rays if they are generated deeper than the average escape depth for that energy. Lithium, for example, has an escape depth of only a few tens of nm. As a result, even a small amount of surface contamination presents extreme challenges to detecting Li with any EDS detector.

As a result, low energy detection is best attained by first using either an ultra-thin, polymer window (<300 nm) or by eliminating the window altogether. Nitrogen gas should not be used to backfill the volume between the thin window and the SDD module if detection below 300 eV is desired. A fully evacuated detector module (or a completely windowless detector) should be employed. Finally, because of X-ray absorption within the sample itself, one should rely primarily on analysis of the top 10–50 nm of the sample. This forces no requirement on the SDD but does imply: (1) extreme care in preparing and in preserving the sample surface and (2) operating the SEM at a shallow penetration depth (<5 kV) to avoid diluting the low energy analysis of the surface region with the high-energy X-rays generated from the overall bulk of the sample.

Energy Resolution and Count Rate

While an energy resolution of 121 eV that pushes the Bremsstrahlung limit is impressive, it is rarely witnessed during normal operation. This energy resolution is typically specified at an input count rate of <5000 counts per second. At these low rates, a peaking time such as 6.4 microseconds can be employed. Shorter peaking times, which are required for high count rate acquisition, result in a greater statistical uncertainty in the energy of the collected X-ray and therefore a lower energy resolution.[2,3] Figure 3 shows the optimal peaking times and resulting impact on energy resolution required to acquire spectra at a maximum dead time of 50%. The energy resolution in this graph changes from 125 eV at 6.4 microseconds up to 175 eV at 0.2 microseconds.

Most mapping applications with an SDD occur at an output count rate of a few hundred thousand counts per second. At a 50% dead time, the ratio of input and output count rates is 2. This ratio will be higher at higher dead times. Mapping at 200,000 input counts/second (100,000 output counts/second), however, results in a resolution degradation of roughly 8 eV at a 1 microsecond time constant. Forced operation at a long time constant prevents this degradation but also results in very slow acquisition rates (few thousand output counts per second) as the very high dead time limits overall throughput. This situation is unsuitable for mapping. A system that allows multiple peaking times, as opposed to only 2 or 3 peaking times, provides a de facto advantage in energy resolution since the longest possible peaking time can be automatically selected for any given input count rate.

The end result is that certain designs may demonstrate an energy resolution of 121 eV at <5000 input counts per second but only achieve an energy resolution of 140–150 eV in mapping mode when output counts exceed 100,000 per second. Thus, a broader specification for energy resolution, which includes both a high- and a low-throughput requirements, would be more useful to the end user.

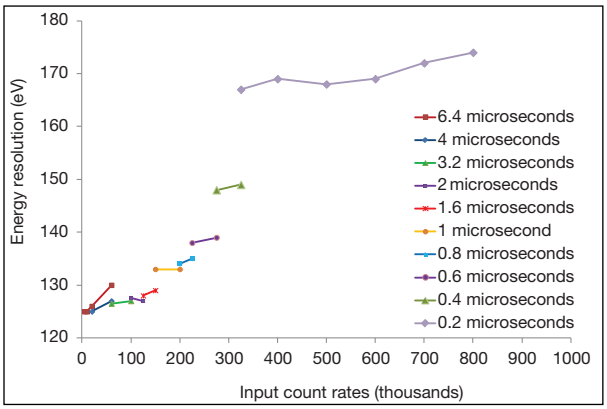

Figure 3: Energy resolution as a function of input count rates at 50% dead time (output count rate is approximately half of input count rate)

Energy Resolution and Post-processing Algorithms

Another consideration related to enhanced energy resolution involves the actual spacing of the X-ray lines generated by the elements within the sample itself. While the spectra in Figures 1 and 2 elegantly present the value of an improved EDS detector, the elements Be, B, C, N, and O all result in single X-ray lines within the spectrum that are separated by 150–250 eV. By comparison, consider the EDS spectrum in Figure 4. The sample analyzed was galena, which is composed primarily of Pb and S with the formula PbS. The S K-line (2.307 keV) and the principal Pb M-line (2.346 keV) are separated by only 39 eV. Furthermore, there are multiple Pb M-lines. The sample was analyzed with two different EDS detectors: (1) the first with an energy resolution of 138 eV and (2) the second with an energy resolution of 122 eV. Finally the sample was also analyzed with a Thermo Scientific™ MagnaRay™ wavelength dispersive spectrometer (WDS). The 122 eV detector spectrum exhibits improvement relative to that of the 138 eV detector. Despite the 16 eV improvement in energy resolution, however, the Pb and S peaks still overlap significantly. No clear distinction between the elemental X-ray lines exists. An energy resolution well below 40 eV would be needed to achieve serious separation of the peaks. Only a WDS, which has superior energy resolution, accurately resolves the S K-line and the Pb M-lines into separate peaks.

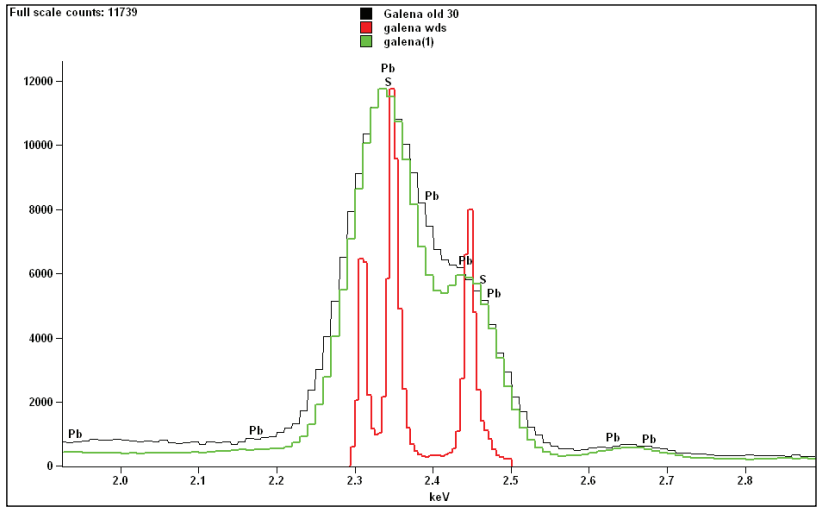

Figure 4: Energy-dispersive X-ray spectrum of galena (primarily Pb and S) for: (a) an SDD at 138 eV (circa 2002), (b) an SDD at 122 eV (circa 2012), and (c) a MagnaRay WDS spectrometer. The principal lines resolved by the WDS are the S Kα at 2.31 keV, the Pb Mα at 2.34 keV, and the combined peak of Pb Mα at 2.44 keV convolved with S Kα at 2.46 keV.

It is clear that the continued presence of closely spaced X-ray lines will always result in overlapping peaks when even the best EDS detector is employed. This prevents direct observation of unidentified specimen elements. This creates not only a challenge to qualitative and quantitative analysis but also to effective element mapping. Fortunately, a solution can be found by the appropriate application of post-processing algorithms.

Figure 5a shows the element maps of the galena sample plotted with "gross" X-ray counts. In other words, with X-ray counts that were not corrected after acquisition. Also shown, for reference, is the WDS element map for Pb and for F. The elements identified as present by the EDS spectrum are Pb, O, F, S, Ca, Mn, Cu, As and Sb. Three regions are evident within the map: (Phase 1) a phase at middle left and middle right comprised mainly of Ca and F; (Phase 2) a phase at center composed mainly of Cu and S; and (Phase 3) a matrix material of Pb and S. The mapped backgrounds are quite high for several elements, including O, Mn, Cu, and As. This indicates either a consistent, low-level distribution of these elements throughout the sample or consistent misidentification of the elements due to peak overlaps within the spectrum. There are also "ghost-like" regions of Ca and Sb in Phase 2. One might dismiss the "ghost-like" Ca and Sb distribution as artifacts. Without further evidence, however, this is a dangerous assumption. In addition, the EDS map for Pb does not match the WDS map for the Pb M-alpha line; another indication that peak overlaps have created errors within the EDS mapping results.

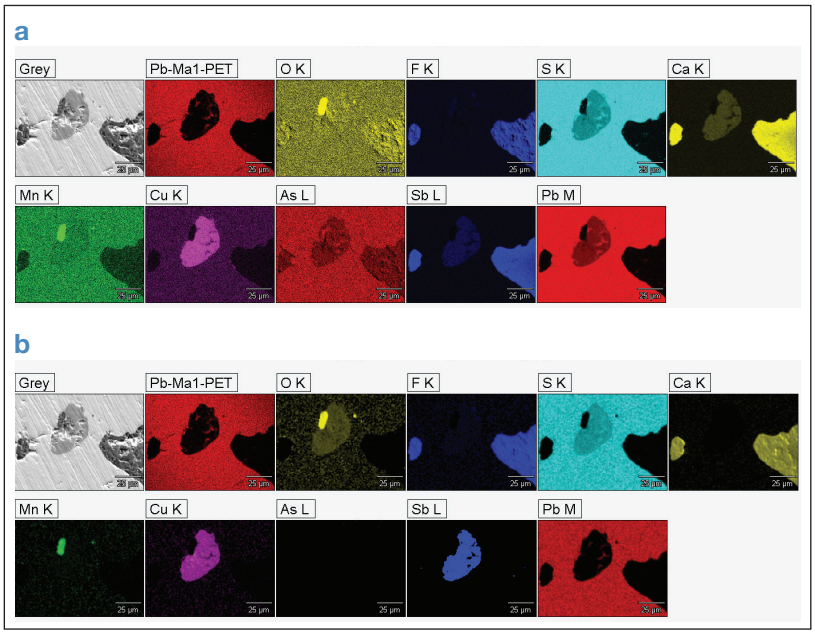

Figure 5: (a) X-ray element maps of galena (PbS) sample exhibiting "gross" or uncorrected X-ray counts, (b) same X-ray element maps of (a) but with corrections for peak deconvolution and background subtraction

Figure 5b shows the same element maps, using the exact same raw data. This time, however, a peak deconvolution, a matrix correction, and a background subtraction algorithm were all applied to the collected spectra in each pixel, colloquially referred to as "quantitative elemental mapping" or "Quant maps". The impact of these maps is immediately evident when the element maps in Figures 5a and 5b are directly compared.

First, the overall image noise around the concentrations of several elements – in particular O, Mn and Cu – falls to zero or near zero except in the actual phase in which it is found to exist. Secondly, the As counts go to zero everywhere. It is now evident that the As, originally identified by the As K-line at 10.532 keV, is indeed an overlap with the Pb L-lines at 10.549 eV. Third, the EDS identification of Pb in the central Cu-S region (i.e., Phase 2) is eliminated; bringing the wt% map of Pb in direct alignment with the WDS map of Pb. Fourth, S still exists in both the central region and the matrix region around it. This helps to clearly identify a Cu and S containing region for Phase 2 surrounded by a Pb-S, or galena, matrix material in Phase 3. Fifth, regarding the Ca and Sb "ghost-like" distributions in Phase 2, the Ca distribution found in the Cu-S region has disappeared completely. The Ca and F are now uniquely isolated to Phase 1 identifying this region as fluorite (CaF_2). Finally, the Quant map clarifies that the Sb, while not present in Phase 1, is indeed present in the Cu-S Phase 2 region. This rejects any hypothesis that the Sb located in this region is an artifact. The presence of Sb in Phase 2 changes the phase type from copper sulfide to chalcostibite ($CuSbS_2$).

This mapping exercise identified six major flaws in a single sample when analyzed using basic mapping techniques and a state-of-the-art, 122 eV resolution, EDS detector. While EDS detectors have advanced significantly in terms of energy resolution over the last decade, it is evident that until energy resolution reaches the level of WDS, efficient post-processing algorithms will remain significantly more important for improving element mapping than any further improvements in energy resolution.

Conclusions

Energy resolution represents only one of many factors in obtaining world-class EDS data. Thin window or windowless technologies and the elimination of any inert gas between the thin window and the SDD crystal are critical to low energy detection. For mapping applications, fast electronics and low capacitance SDDs are critical to minimizing the degradation in energy resolution that necessarily occurs at output counts rates of a few hundred thousand per second. Finally, while an extreme EDS energy resolution generates aesthetically pleasing spectra, powerful post-processing algorithms provide the most powerful lever (short of full WDS element mapping) for producing high-quality, accurate EDS elemental maps. While EDS detectors have advanced significantly in over the last 15 years, the energy resolution specification now approaches the limits of physics. Other developments in EDS now take up the work of improving EDS data collection and analysis.

References

1. Goldstien et al., pages 311–312, Scanning Electron Microscopy and X-ray Microanalysis, Springer, New York, 2003
2. L. Strueder, N. Meidinger, D. Stotter, J. Kemmer, P. Lechner, P. Leutenegger, H. Soltau, F. Eggert, M. Rohde, T. Schulein, High Resolution X-Ray Spectroscopy Close to Room Temperature, July 1998
3. Amptek Silicon Drift Diode (SDD) at High Count Rates, AN-SDD-001 Rev B0, http://www.amptek.com

Africa +27 11 822 4120
Australia +61 3 9757 4300
Austria +43 1 333 50 34 0
Belgium +32 53 73 42 41
Canada +1 800 530 8447
China +86 10 8419 3588
Denmark +45 70 23 62 60
Europe-Other +43 1 333 50 34 0
Finland/Norway/Sweden +46 8 556 468 00
France +33 1 60 92 48 00
Germany +49 6103 408 1014
India +91 22 6742 9434
Italy +39 02 950 591
Japan +81 45 453 9100
Latin America +1 561 688 8700
Middle East +43 1 333 50 34 0
Netherlands +31 76 579 55 55
New Zealand +64 9 980 6700
Russia/CIS +43 1 333 50 34 0
Spain +34 914 845 965
Switzerland +41 61 716 77 00
UK +44 1442 233555
USA +1 800 532 4752

Thermo SCIENTIFIC
Part of Thermo Fisher Scientific

TN52537_E 10/13M